

1 **The analysis of the long-term impact of SARS-CoV-2 on the cellular immune**
2 **system in individuals recovering from COVID-19 reveals a profound NKT cell**
3 **impairment**

4 Jia Liu^{1,3*#}, Xuecheng Yang^{1,3*}, Hua Wang¹, Ziwei Li^{1,3}, Hui Deng^{1,3}, Jing Liu^{1,3}, Shue
5 Xiong^{1,3}, Junyi He^{1,3}, Chunxia Guo¹, Weixian Wang¹, Gennadiy Zelinskyy^{2,3}, Mirko
6 Trilling^{2,3}, Ulf Dittmer^{2,3}, Mengji Lu^{2,3}, Kathrin Sutter^{2,3}, Tina Senff⁴, Christopher
7 Menne⁴, Joerg Timm⁴, Yanfang Zhang⁵, Fei Deng⁵, Xuemei Feng^{1,3}, Yinping Lu^{1,3},
8 Jun Wu^{1,3}, Dongliang Yang^{1,3}, Baoju Wang^{1,3#}, Xin Zheng^{1,3}

9

10 ¹ *Department of Infectious Diseases, Union Hospital, Tongji Medical College,*
11 *Huazhong University of Science and Technology, Wuhan 430022, China*

12 ² *Institute for Virology, University Hospital of Essen, University of Duisburg-Essen,*
13 *Essen 45147, Germany*

14 ³ *Joint International Laboratory of Infection and Immunity, Huazhong University of*
15 *Science and Technology, Wuhan 430022, China*

16 ⁴ *Institute for Virology, Heinrich-Heine-University, University Hospital, Duesseldorf*
17 *40225, Germany*

18 ⁵ *Wuhan Institute of Virology, Chinese Academy of Sciences, Wuhan, China*

19

20

21 * # These authors contributed equally to this work.

22

23 **Correspondence to:**

24 Prof. Dr. Jia Liu, e-mail: jialiu77@hust.edu.cn

25 Tel: +8618696159826

26 Department of Infectious Diseases, Union Hospital, Tongji Medical College,

27 Huazhong University of Science and Technology, Wuhan 430022, China

28

29 Prof. Dr. Baoju Wang, e-mail: bjwang73@163.com

30 Tel: +8613627288476

31 Department of Infectious Diseases, Union Hospital, Tongji Medical College,

32 Huazhong University of Science and Technology, Wuhan 430022, China

33 **ABSTRACT**

34 The *coronavirus disease 2019* (COVID-19) pandemic caused by the *severe acute*
35 *respiratory syndrome coronavirus 2* (SARS-CoV-2) affects millions of people and
36 killed hundred-thousands of individuals. While acute and intermediate interactions
37 between SARS-CoV-2 and the immune system have been studied extensively,
38 long-term impacts on the cellular immune system remained to be analyzed. Here, we
39 comprehensively characterized immunological changes in peripheral blood
40 mononuclear cells in 49 COVID-19 convalescent individuals (CI) in comparison to 27
41 matched SARS-CoV-2 unexposed individuals (UI). Despite recovery from the disease
42 for more than 2 months, CI showed significant decreases in frequencies of invariant
43 NKT and NKT-like cells compared to UI. Concomitant with the decrease in NKT-like
44 cells, an increase in the percentage of Annexin V and 7-AAD double positive
45 NKT-like cells was detected, suggesting that the reduction in NKT-like cells results
46 from cell death months after recovery. Significant increases in regulatory T cell
47 frequencies, TIM-3 expression on CD4 and CD8 T cells, as well as PD-L1 expression
48 on B cells were also observed in CI, while the cytotoxic potential of T cells and
49 NKT-like cells, defined by GzmB expression, was significantly diminished. However,
50 both CD4 and CD8 T cells of CI showed increased Ki67 expression and were fully
51 capable to proliferate and produce effector cytokines upon TCR stimulation.
52 Collectively, we provide the first comprehensive characterization of immune
53 signatures in patients recovering from SARS-CoV-2 infection, suggesting that the
54 cellular immune system of COVID-19 patients is still under a sustained influence

55 even months after the recovery from disease.

56 **Introduction**

57 The sudden emergence and rapid global spread of *severe acute respiratory syndrome*
58 *coronavirus 2* (SARS-CoV-2) and the resulting *coronavirus disease 2019* (COVID-19)
59 poses an unprecedented health crisis to humankind. As of August 14th, 2020, there
60 were more than 20 million documented cases of SARS-CoV-2 infection and more
61 than 750 thousand individuals lost their lives. SARS-CoV-2-infected people exhibit a
62 wide spectrum of disease manifestations ranging from moderate or even unnoticed
63 symptoms (1) to life-threatening acute infections predominantly affecting the
64 respiratory tract (2) but also other organs such as the kidney (3) and the central
65 nervous system (4) can be harmed. Moderate cases show symptoms of fever, dry
66 cough, fatigue, abnormal chest CT findings but with a good prognosis (5, 6).
67 Conversely, some patients suddenly deteriorate towards acute respiratory distress
68 syndrome (ARDS) or multiple organ failure, with fatality rates approaching 60% (7).

69 Recent studies demonstrated that SARS-CoV-2 infections strongly shape the immune
70 system and result in its dysregulation, including imbalanced antiviral and
71 pro-inflammatory responses, altered numbers and impaired functions of different
72 immune cell subsets (8). We and others previously showed that lymphopenia and an
73 inflammatory cytokine storm can be observed in COVID-19 patients and that their
74 extents correlate with COVID-19-associated disease severity and mortality (9-12).
75 The recovery of T cell counts and the end of the inflammatory cytokine storm in
76 severe COVID-19 cases have been associated with a favorable disease outcome (9).
77 However, the impact of SARS-CoV-2 on the cellular immune system after the

78 recovery from the disease remains largely unknown.

79 Applying multi-color flow cytometry, we comprehensively characterized
80 immunological changes in peripheral blood mononuclear cells (PBMCs) in 49
81 convalescent SARS-CoV-2-infected individuals (CI) in comparison to 27 matched
82 SARS-CoV-2-unexposed individuals (UI). To our knowledge, our results provide the
83 first in-depth description of immune signatures in the aftermath of SARS-CoV-2
84 infections in convalescent patients. Our data suggest that the immune system remains
85 heavily influenced months after resolving SARS-CoV-2 infection.

86

87 **Methods**

88 **Subjects**

89 Thirty convalescent individuals who resolved their SARS-CoV-2 infection and a
90 matched group comprising 21 SARS-CoV-2-unexposed individuals were recruited at
91 the Department of Infectious Diseases, Union Hospital, Tongji Medical College,
92 Huazhong University of Science and Technology and the Department of
93 Gastroenterology from May to June 2020. The diagnosis of COVID-19 was based on
94 the Guidelines for Diagnosis and Treatment of Corona Virus Disease 2019 issued by
95 the National Health Commission of China (7th edition,
96 http://www.chinacdc.cn/jkzt/crb/zl/szkb_11803/jszl_11815/202003/t20200305_21414
97 2.html). Informed written consent was obtained from each patient and the study
98 protocol was approved by the local medical ethics committee of Union Hospital,
99 Tongji Medical College, Huazhong University of Science and Technology in
100 accordance with the guidelines of the Declaration of Helsinki (2020IEC-J-587).
101 Invariant NKT cell analysis was performed in a German cohort which has 19 CI and 6
102 UI. Written informed consent was given from each included individual and the study
103 was approved by the ethics committee of medical faculty of the Heinrich Heine
104 University Düsseldorf Germany (study number: 5350).

105

106 **Preparation of PBMCs**

107 Peripheral blood mononuclear cells (PBMCs) of SARS-CoV-2-unexposed individuals

108 and patients were isolated using Ficoll density gradient centrifugation (DAKEWE
109 Biotech, Beijing) and were rapidly assessed by flow cytometry analysis without
110 intermittent cryo-conservation.

111

112 **Flow cytometry**

113 Surface and intracellular staining for flow cytometry analysis were performed as
114 described previously(13, 14). For surface staining, cells were incubated with relevant
115 fluorochrome-labeled antibodies for 30 min at 4°C in the dark. For intracellular
116 cytokine staining, cells were fixed and permeabilized using the Intracellular Fixation
117 & Permeabilization Buffer Set (Invitrogen, USA) and stained with APC-anti-IFN- γ ,
118 PerCP-Cy5.5-anti-IL-2, or FITC-anti-TNF α (BD Biosciences, USA). Freshly isolated
119 cells were used for all assays. Approximately 100,000 PBMCs were acquired for each
120 sample using a BD FACS Canto II flow cytometer. Data analysis was performed using
121 FlowJo software V10.0.7 (Tree Star, Ashland, OR, USA). Cell debris and dead cells
122 were excluded from the analysis based on scatter signals and Fixable Viability Dye
123 eFluor 506.

124

125 **Analysis of effector T cell responses**

126 PBMCs were resuspended in complete medium (RPMI 1640 containing 10% fetal
127 calf serum, 100U/ml penicillin, 100 μ g/ml streptomycin, and 100 μ M
128 4-[2-hydroxyethyl]-1-piperazine ethanesulfonic acid buffer) and stimulated with

129 anti-CD3 (1 μ g/ml; BD Biosciences, USA), anti-CD28 (1 μ g/ml; BD Biosciences,
130 USA), and recombinant interleukin-2 (20U/ml; Hoffmann-La Roche, Italy). Fresh
131 medium containing IL-2 was added every 72 hours. On day 5, brefeldin A (BD
132 Biosciences, San Diego, CA) was added to the media for 6 hours. Cells were washed
133 and tested for Ki67 expression and secretion of IFN- γ , IL-2, and TNF- α by
134 intracellular cytokine staining and subsequent flow cytometry analyses.

135

136 **Statistical Analysis**

137 Statistics comparing two groups were done using the Mann-Whitney t-test. When
138 more than two groups were compared, a one-way ANOVA was used with a Tukey
139 post-hoc test (GraphPad Prism software; GraphPad Software Inc., San Diego, USA).

140

141 **Results**

142 *Characteristics of the study cohort*

143 To characterize the cellular immune system in individuals that had recovered from
144 COVID-19, blood samples were analyzed about 3.5 months (Chinese cohort) or 1.5
145 months (German cohort) after the first diagnosis. The demographic profiles of the
146 Chinese cohort are shown in Table 1. All CI had been diagnosed as either moderate
147 (83.3%, 25/30) or mild COVID-19 cases (16.7%, 5/30). The median period between
148 the first diagnosis of COVID-19 and blood sampling was 112 days (range: 60 to 136
149 days). Among all COVID-19 cases, 43.3% (13/30) were hospitalized and 23.3% (7/30)
150 received oxygen inhalation treatment. Leukopenia and lymphopenia were observed in
151 43.5% (10/23) and 60.9% (14/23) of tested cases, respectively. Increased C-reactive
152 protein and IL-6 levels were observed in 52.6% (10/19) and 76.9% (10/13) of tested
153 patients, respectively. All moderate cases showed abnormal radiological findings
154 suggesting pneumonia by chest computed tomography (CT) scans, while mild cases
155 showed no radiological abnormality in the lungs. Twelve moderate cases and one mild
156 case (43.3%, 13/30) had positive RT-PCR results for viral RNA. All patients were
157 anti-SARS-CoV-2 IgM and/or IgG seropositive. At the time of blood sampling, 20%
158 (6/30) of cases exhibited virus-specific IgM and IgG, 70% (21/30) were IgG single
159 positive, and 10% (3/30) were IgM and IgG negative. The demographic profiles of the
160 German cohort are shown in Table 2. This cohort has 19 CI, in which 10.53 % (2/19)
161 were hospitalized. Nine cases (47.37%, 9/19) had positive RT-PCR results for viral
162 RNA, and 18 cases (94.74%, 18/19) were anti-SARS-CoV-2 IgA and/or IgG

163 seropositive. The median period between the first diagnosis of COVID-19 and blood
164 sampling in the German cohort was 41 days. Only the analysis of invariant NKT
165 (iNKT) cells was performed in the German cohort, while analysis of all other cell
166 populations was performed in the Chinese cohort.

167

168 The criteria for COVID-19 convalescent are as follows: afebrile for more than 3 days,
169 resolution of respiratory symptoms, substantial improvement of chest CT images and
170 two consecutive negative RT-qPCR tests for viral RNA in respiratory tract swab
171 samples obtained at least 24 h apart. At time of blood sampling, all CI were negative
172 for viral RNA test and had no recognized medical conditions.

173

174 *Characterization of immune cell subsets in individuals recovering from COVID-19*

175 First, we characterized whether the overall immune cell composition in PBMCs differ
176 between CI and UI by flow cytometry (as depicted in figure S1A and S1B). We
177 observed that the profile of the immune cell composition of CI was distinct from that
178 of UI (Figure 1A). Specifically, the frequencies but not the absolute numbers of CD4+
179 T cells in CI were slightly but significantly higher than in UI (Figure 1B and S1C),
180 while no significant differences in absolute numbers and frequencies of total T cells,
181 CD8+ T cells, B cells, NK cells, and monocytes were observed between CI and UI
182 (Figure 1B and S1C). Interestingly, CI showed dramatic decreases in frequencies of
183 both the NKT-like cell population (CD3+ CD56+) and the iNKT cell population

184 (α -GalCer-CD1d tetramer+ and TCR V α 24-V β 11+) compared to UI (Figure 1C and
185 1D). The absolute numbers of NKT-like cells of CI (median: 20.7/ μ l) were only about
186 60% of the level observed in UI (median: 34.5/ μ l, figure 1C). Besides, CI showed a
187 significant increase in dendritic cells (DCs) in both the absolute numbers and
188 frequencies compared to UI (Figure 1E).

189 Next, we examined whether the decrease of NKT-like cells in CI was associated with
190 increased cell death. Annexin V and 7-AAD stainings were performed to analyze
191 apoptosis and necroptosis of NKT-like cells, CD4 and CD8 T cells, B cells, and NK
192 cells. A profound and significant increase in the frequency of the Annexin V and
193 7-AAD double positive NKT-like cells was observed in CI (median: 3.3%) compared
194 to UI (median: 1.2%) (Figure 2A), suggesting that increased proportions of NKT-like
195 cells of CI are undergoing apoptosis and/or necroptosis even after recovery from
196 COVID-19. Importantly, the intensities of NKT-like cell death were inversely
197 correlated with NKT cell frequencies in CI (Figure 2B). Besides, apoptosis and/or
198 necroptosis of CD4+ T cells and B cells were also slightly increased in CI compared
199 to those in UI (Figure 2C).

200 Taken together, these results demonstrate that SARS-CoV-2 infections elicit a
201 sustained impact on the immune cell composition in the peripheral blood during the
202 extended convalescence phase, dominated by a contraction of NKT-like cells, and an
203 expansion of DCs.

204

205 ***Characterization of T cell phenotypes in individuals recovering from COVID-19***

206 Next, we used several markers of CD4 and CD8 T cells to determine their
207 differentiation (CD45RA and CCR7), proliferation (Ki67), activation (CD38 and
208 HLA-DR), and exhaustion / suppression (PD-1, TIM-3, TOX, and Tregs) status. We
209 also defined different subpopulations and T cells from UI and CI were divided into
210 naïve (CD45RA+ CCR7+), central memory (TCM, CD45RA- CCR7+), effector
211 memory (TEM, CD45RA- CCR7-), and terminally differentiated effector (TEMRA,
212 CD45RA+ CCR7-) subpopulations (Figure S2). No significant differences were
213 observed between UI and CI for any of the CD4 or CD8 T cell subpopulations
214 mentioned above, although a tendency of decreased CD4+ TEMRA cell frequencies
215 in CI (median: 3.3%) compared to UI (median: 7.5%) was observed (Figure S2). The
216 proliferation (Ki67+) expression of both CD4 and CD8 T cells in CI was higher than
217 that in UI (median: CD4 3.8% vs 2.7%, CD8 2.5% vs 1.9%), and the difference for
218 CD8 T cells was statistically significant (Figure 3A), indicating that T cells from CI
219 show an enhanced proliferation capacity. Previous studies have shown that T cells are
220 highly activated during the acute phase of COVID-19 (15), thus we next analyzed the
221 activation status of CD4 and CD8 T cells by examining CD38 and HLA-DR
222 expression on the cell surface. No significant differences in CD38 and HLA-DR
223 expression on CD4 T cells were observed between UI and CI (Figure 3B and S3A).
224 Compared to UI, CI showed 1.47-fold increase in the frequencies of CD38+
225 HLA-DR- CD8 T cells, however, this difference was not statistically significant
226 (Figure 3C and S3A). Based on the analysis of PD-1 expression, some studies

227 reported that CD8 T cells may already become functionally exhausted during the
228 acute phase of COVID-19 (16), which was questioned by a different study from our
229 group (Westmeier J, et al. In submission). In our current study, the PD-1 expression
230 levels on CD4 or CD8 T cells from CI were similar to those in UI (Figure 3B, 3C and
231 S3B). However, the expression of TIM-3, another immune check point molecule, was
232 increased about 20% on CD4 and CD8 T cells in CI compared to UI, and this
233 difference was statistically significant (Figure 3D). Moreover, we examined the
234 expression of TOX in T cells from our study subjects, which is a newly identified key
235 factor of T cell exhaustion (17, 18). The frequencies of TOX+ CD4 and CD8 T cells
236 in CI increased around 20-30% compared to those in UI, however, the differences
237 were not statistically significant (Figure 3B, 3C and S3B). Regulatory T cells (Tregs)
238 play a very important role in controlling immunopathogenic reactions upon infections
239 by dampening pathogen-specific immune responses (19-21). We therefore examined
240 the frequencies of Tregs in the PBMCs of CI by analyzing Foxp3 expression in CD4 T
241 cells. As shown in figure 3E, CI showed a significant increase in Tregs frequencies
242 (median: 8.8%) compared to those in UI (median: 6.8%).

243 Taken together, our results demonstrate an immune environment that is prone towards
244 T cell suppression during the late COVID-19 convalescent phase. However, T cells in
245 CI still show a slightly enhanced activation and proliferation status, suggesting that
246 these individuals are situated in a phase of ongoing restoration of the immune
247 homeostasis.

249 ***Characterization of cytotoxic effector profiles of T, NK, and NKT-like cells in***
250 ***individuals recovering from COVID-19***

251 To characterize their cytotoxic profiles, we intracellularly stained CD4, CD8,
252 NKT-like, and NK cells for the cytotoxic molecules Granzyme B (GzmB) and
253 perforin directly *ex vivo* without re-stimulation and compared UI with CI. CI showed
254 significant decreases in the frequencies of GzmB-producing NKT-like cells (median:
255 53.2%) and CD8 T cells (mean: 20.3%) compared to UI (NKT-like cells: 81.2%, CD8
256 T cells: 29.8%, figure 4A-4D). A tendency of decreased frequencies of
257 GzmB-producing CD4 T cells was also observed, however, this difference was not
258 statistically significant (Figure 4E and 4F). Consistently, the level (mean fluorescence
259 intensity; MFI) of GzmB expression in individual NKT-like, CD4 and CD8 T cells
260 was also significantly lower in CI than in UI (Figure 4A-4F). However, we did not
261 observe significant differences in GzmB expression in NK cells. Interestingly,
262 perforin expression was not different for all analyzed cell populations between CI and
263 UI (Figure S4). We also examined the production of inflammatory cytokines such as
264 interferon- γ (IFN- γ), IL-6, and granulocyte-macrophage colony-stimulating factor
265 (GM-CSF) by T cells, NK cells, and NKT-like cells in CI, since a previous study
266 demonstrated that significant numbers of T cells produce these cytokines during the
267 acute phase of COVID-19 (22). Although certain increases in the frequencies of CD4
268 and CD8 T cells producing IFN- γ , IL-6, and GM-CSF were observed in CI compared
269 to UI (Figure 4C and 4E), these differences were not statistically significant and
270 appeared to be affected by two outliers in the CI group that had profound numbers of

271 cytokine-producing T cells (Figure S4B and S4C). No significant differences in
272 frequencies of IFN- γ , IL-6 and GM-CSF producing NK and NKT-like cells were
273 observed between CI and UI (Figure S4A and S4F).

274 To further characterize effector functions of T cells in response to TCR stimulation.
275 PBMCs from 5 CI and 5 UI were stimulated with anti-CD3/anti-CD28 for 5 days and
276 were examined for cell proliferation (Ki67) and effector cytokine expression (IFN- γ ,
277 IL-2, and TNF- α). Compared to unstimulated cells, anti-CD3/anti-CD28 stimulation
278 induced expected increases of Ki67 expression, as well as IFN- γ , IL-2, and TNF- α
279 production of CD4 and CD8 T cells in both CI and UI (Figure 5). No significant
280 differences in effector cytokine production or proliferation of CD4 and CD8 T cells
281 were observed between the groups (Figure 5B-5D).

282 Taken together, these results indicate that there is a long-term suppression of the
283 cytotoxic potential of T cells after resolving SARS-CoV-2 infection, however, general
284 effector functions of T cells in COVID-19 convalescent individuals are maintained.

285

286 ***Phenotype of antigen presenting cells in individuals recovering from COVID-19***

287 Next, we evaluated the phenotype and functional properties of antigen presenting cells
288 (APCs), including DCs, B cells, and monocytes by analyzing their CD80, CD86,
289 CD72, and PD-L1 expression and compared UI with CI. DCs of CI showed about 20%
290 increased CD80 expression intensities on the cell surface compared to those of UI and
291 this difference was statistically significant (Figure 6A and 6B). CD80 and PD-L1

292 expression significantly increased by about 20% and CD72 by about 50% on the
293 surface of B cells of CI (Figure 6C and 6D). No significant differences in CD86,
294 CD72, and PD-L1 expression on DCS, CD86 on B cells, and CD80, CD86, CD72,
295 and PD-L1 on monocytes were observed between the groups (Figure S5). Taken
296 together, increased expression of costimulatory molecules on DCs and B cells
297 suggests that APCs in CI are at a slightly enhanced activation status.

298

299 **Discussion**

300 Wuhan was the very first city hit by SARS-CoV-2. Accordingly, the patients who
301 experienced the longest phase of convalescence following COVID-19 reside here.
302 This enabled us to investigate the ‘immunological scar’ left by SARS-CoV-2 on
303 cellular immunity after recovery from the disease. Our results reveal that 2 to 4
304 months after resolved SARS-CoV-2 infection, most components of cellular immunity
305 returned to normal. However, the previous SARS-CoV-2 infection could still be
306 recognized during convalescent phase by diminished numbers of NKT-like cells and
307 iNKT cells as well as increased DCs. CIs show an immune environment prone to
308 suppression, supporting by the observation of significantly increases Treg frequencies,
309 and upregulation of TIM-3 expression on T cells, and PD-L1 expression on B cells.
310 Accordingly, the cytotoxic potential, as represented by GzmB expression, of T cells
311 and NKT-like cells was significantly suppressed in CIs. Both CD4 and CD8 T cells of
312 CIs showed increased cell proliferation and were fully capable of producing effector
313 cytokines in response to TCR stimulation, suggesting the effector function of T cells
314 is not compromised in CIs.

315 Unexpectedly, our study revealed profound changes of NKT cells in the convalescent
316 phase of COVID-19. NKT cells are a small but important subset of T lymphocytes
317 that regulate immune responses in the context of infection, cancer, and autoimmunity
318 (23). NKT cells can promote cell-mediated immunity to tumors and pathogens, yet
319 they can also suppress the cell-mediated immunity associated with autoimmune
320 diseases and are involved in the pathogenesis of many inflammatory disorders (24).

321 NKT-like cells were shown to be cytotoxic toward lung epithelial cells and involved
322 in the immunopathogenesis of pulmonary disease (25). It remains unclear by which
323 means NKT cells carry out such opposing functions. The existence of functionally
324 distinct NKT cell subsets may provide a rational explanation: so far, 3 NKT cell
325 subsets, including classical NKT cells (iNKT cells), non-classical NKT cells, and
326 NKT-like cells, each expressing different TCRs have been described (26). These cells
327 are activated by lipid antigens linked to non-polymorphic CD1 molecules and/or
328 pro-inflammatory cytokines generated during infection, and significantly contribute to
329 the onset of infectious or autoimmune diseases (27). Reduced numbers of iNKT cells
330 among PBMCs appear to correlate with the activity of systemic lupus erythematosus
331 (SLE) disease (28). Selective loss of iNKT cells has also been reported during acute
332 lymphocytic choriomeningitis virus (LCMV) infections (29), as well as in chronic
333 HIV and UIV infection (30-32). Interestingly, subsequent long-term loss of iNKT
334 cells during the convalescent phase following acute LCMV infection of mice has also
335 been reported (33). It is believed that the reduction in iNKT cells at these late stages
336 post-infection occurred by activation-induced cell death, since concomitant with the
337 decrease in iNKT cells was an increase in the frequency of Annexin V+ iNKT cells
338 (33). Highly similar to the observation in acute LCMV infections of mice, we also
339 demonstrate a selective long-term loss of iNKT and NKT-like cells three months after
340 recovering from an acute SARS-CoV-2 infection. The observation of increases in the
341 frequency of Annexin V+ NKT-like cells in convalescent individuals suggests that the
342 reduction of these cells may also occurred by activation-induced cell death. Recent

343 studies have reported that during acute SARS-CoV-2 infection, NKT-like cells
344 showed a significant increase in GzmB and perforin production (34), as well as a
345 decrease in numbers in severe COVID-19 cases (35), suggesting these cells are highly
346 activated during the acute phase. A very recent study has also demonstrated the
347 expansion of NKT CD160 cluster in moderate but not severe COVID-19 patients,
348 which was believed to promote rapid control of the disease through direct cytotoxicity
349 as well as mediating the antibody-dependent cell-mediated cytotoxicity effect (36).
350 Taken together, these data suggest that the activation and subsequent long-term loss of
351 NKT and NKT-like cells during COVID-19 is a normal component of the host's
352 antiviral immune response. The mechanisms that regulate numbers and functions of
353 NKT and NKT-like cells following SARS-CoV-2 infection should be further
354 investigated.

355 In summary, we characterized the long-term impact of SARS-CoV-2 infection on the
356 immune system and provide comprehensive picture of cellular immunity of a
357 convalescent COVID-19 patient cohort with the longest recovery time. The overall
358 alterations affecting cellular immunity observed in this study suggests that the
359 immune system in convalescent individuals is going through a phase of restoring
360 homeostasis after being highly activated during the acute phase of SARS-CoV-2
361 infection.

362 **Acknowledgement**

363 This work is supported by the Fundamental Research Funds for the Central
364 Universities (2020kfyXGYJ028, 2020kfyXGYJ046 and 2020kfyXGYJ016), the
365 National Natural Science Foundation of China (81861138044 and 91742114), the
366 National Science and Technology Major Project (2017ZX10202203), and the Medical
367 Faculty of the University of Duisburg-Essen and Stiftung Universitaetsmedizin,
368 University Hospital Essen, Germany.

369

370

371 **References**

- 372 1. Long QX, Tang XJ, Shi QL, Li Q, Deng HJ, Yuan J, Hu JL, Xu W, Zhang Y,
373 Lv FJ, et al. Clinical and immunological assessment of asymptomatic
374 SARS-CoV-2 infections. *Nature medicine*. 2020.
- 375 2. Guan WJ, Ni ZY, Hu Y, Liang WH, Ou CQ, He JX, Liu L, Shan H, Lei CL,
376 Hui DSC, et al. Clinical Characteristics of Coronavirus Disease 2019 in China.
377 *The New England journal of medicine*. 2020;382(18):1708-20.
- 378 3. Puelles VG, Lutgehetmann M, Lindenmeyer MT, Sperhake JP, Wong MN,
379 Allweiss L, Chilla S, Heinemann A, Wanner N, Liu S, et al. Multiorgan and
380 Renal Tropism of SARS-CoV-2. *The New England journal of medicine*.
381 2020;383(6):590-2.
- 382 4. Asadi-Pooya AA, and Simani L. Central nervous system manifestations of
383 COVID-19: A systematic review. *Journal of the neurological sciences*.
384 2020;413(116832).
- 385 5. Huang C, Wang Y, Li X, Ren L, Zhao J, Hu Y, Zhang L, Fan G, Xu J, Gu X, et
386 al. Clinical features of patients infected with 2019 novel coronavirus in Wuhan,
387 China. *Lancet*. 2020.
- 388 6. Chan JF, Yuan S, Kok KH, To KK, Chu H, Yang J, Xing F, Liu J, Yip CC,
389 Poon RW, et al. A familial cluster of pneumonia associated with the 2019
390 novel coronavirus indicating person-to-person transmission: a study of a
391 family cluster. *Lancet*. 2020.
- 392 7. Yang X, Yu Y, Xu J, Shu H, Xia J, Liu H, Wu Y, Zhang L, Yu Z, Fang M, et al.
393 Clinical course and outcomes of critically ill patients with SARS-CoV-2
394 pneumonia in Wuhan, China: a single-centered, retrospective, observational
395 study. *The Lancet Respiratory medicine*. 2020;8(5):475-81.
- 396 8. Vabret N, Britton GJ, Gruber C, Hegde S, Kim J, Kuksin M, Levantovsky R,
397 Malle L, Moreira A, Park MD, et al. Immunology of COVID-19: Current State
398 of the Science. *Immunity*. 2020.
- 399 9. Liu J, Li S, Liu J, Liang B, Wang X, Wang H, Li W, Tong Q, Yi J, Zhao L, et
400 al. Longitudinal characteristics of lymphocyte responses and cytokine profiles
401 in the peripheral blood of SARS-CoV-2 infected patients. *EBioMedicine*.
402 2020;55(102763).

- 403 10. Wang D, Hu B, Hu C, Zhu F, Liu X, Zhang J, Wang B, Xiang H, Cheng Z,
404 Xiong Y, et al. Clinical Characteristics of 138 Hospitalized Patients With 2019
405 Novel Coronavirus-Infected Pneumonia in Wuhan, China. *Jama*. 2020.
- 406 11. Mehta P, McAuley DF, Brown M, Sanchez E, Tattersall RS, Manson JJ, and
407 Hlh Across Speciality Collaboration UK. COVID-19: consider cytokine storm
408 syndromes and immunosuppression. *Lancet*. 2020;395(10229):1033-4.
- 409 12. Moore JB, and June CH. Cytokine release syndrome in severe COVID-19.
410 *Science*. 2020;368(6490):473-4.
- 411 13. Liu J, Jiang M, Ma Z, Dietze KK, Zelinskyy G, Yang D, Dittmer U, Schlaak
412 JF, Roggendorf M, and Lu M. TLR1/2 ligand-stimulated mouse liver
413 endothelial cells secrete IL-12 and trigger CD8+ T cell immunity in vitro.
414 *Journal of immunology (Baltimore, Md : 1950)*. 2013;191(12):6178-90.
- 415 14. Wang Q, Pan W, Liu Y, Luo J, Zhu D, Lu Y, Feng X, Yang X, Dittmer U, Lu
416 M, et al. Hepatitis B Virus-Specific CD8+ T Cells Maintain Functional
417 Exhaustion after Antigen Reexposure in an Acute Activation Immune
418 Environment. *Frontiers in immunology*. 2018;9(219).
- 419 15. Zheng HY, Zhang M, Yang CX, Zhang N, Wang XC, Yang XP, Dong XQ, and
420 Zheng YT. Elevated exhaustion levels and reduced functional diversity of T
421 cells in peripheral blood may predict severe progression in COVID-19 patients.
422 *Cellular & molecular immunology*. 2020;17(5):541-3.
- 423 16. Diao B, Wang C, Tan Y, Chen X, Liu Y, Ning L, Chen L, Li M, Liu Y, Wang G,
424 et al. Reduction and Functional Exhaustion of T Cells in Patients With
425 Coronavirus Disease 2019 (COVID-19). *Front Immunol*. 2020;11(827).
- 426 17. Alfei F, Kanev K, Hofmann M, Wu M, Ghoneim HE, Roelli P, Utzschneider
427 DT, von Hoesslin M, Cullen JG, Fan Y, et al. TOX reinforces the phenotype
428 and longevity of exhausted T cells in chronic viral infection. *Nature*.
429 2019;571(7764):265-9.
- 430 18. Khan O, Giles JR, McDonald S, Manne S, Ngiow SF, Patel KP, Werner MT,
431 Huang AC, Alexander KA, Wu JE, et al. TOX transcriptionally and
432 epigenetically programs CD8(+) T cell exhaustion. *Nature*.
433 2019;571(7764):211-8.
- 434 19. Belkaid Y. Role of Foxp3-positive regulatory T cells during infection. *Eur J*
435 *Immunol*. 2008;38(4):918-21.

- 436 20. Zelinsky G, Dietze KK, Husecken YP, Schimmer S, Nair S, Werner T,
437 Gibbert K, Kershaw O, Gruber AD, Sparwasser T, et al. The regulatory T-cell
438 response during acute retroviral infection is locally defined and controls the
439 magnitude and duration of the virus-specific cytotoxic T-cell response. *Blood*.
440 2009;114(15):3199-207.
- 441 21. Hasenkrug KJ, Chougnet CA, and Dittmer U. Regulatory T cells in retroviral
442 infections. *PLoS pathogens*. 2018;14(2):e1006776.
- 443 22. Zhou Y, Fu B, Zheng X, Wang D, Zhao C, Qi Y, Tian Z, Xu X, and Wei H.
444 Pathogenic T-cells and inflammatory monocytes incite inflammatory storms in
445 severe COVID-19 patients. *National Science Review*. 2020;6(998-1002).
- 446 23. Slauenwhite D, and Johnston B. Regulation of NKT Cell Localization in
447 Homeostasis and Infection. *Frontiers in immunology*. 2015;6(255).
- 448 24. Godfrey DI, Stankovic S, and Baxter AG. Raising the NKT cell family. *Nature*
449 *immunology*. 2010;11(3):197-206.
- 450 25. Hodge G, and Hodge S. Steroid Resistant CD8(+)CD28(null) NKT-Like
451 Pro-inflammatory Cytotoxic Cells in Chronic Obstructive Pulmonary Disease.
452 *Frontiers in immunology*. 2016;7(617).
- 453 26. Godfrey DI, MacDonald HR, Kronenberg M, Smyth MJ, and Van Kaer L.
454 NKT cells: what's in a name? *Nature reviews Immunology*. 2004;4(3):231-7.
- 455 27. Torina A, Guggino G, La Manna MP, and Sireci G. The Janus Face of NKT
456 Cell Function in Autoimmunity and Infectious Diseases. *Int J Mol Sci*.
457 2018;19(2).
- 458 28. Cho YN, Kee SJ, Lee SJ, Seo SR, Kim TJ, Lee SS, Kim MS, Lee WW, Yoo
459 DH, Kim N, et al. Numerical and functional deficiencies of natural killer T
460 cells in systemic lupus erythematosus: their deficiency related to disease
461 activity. *Rheumatology*. 2011;50(6):1054-63.
- 462 29. Hobbs JA, Cho S, Roberts TJ, Sriram V, Zhang J, Xu M, and Brutkiewicz RR.
463 Selective loss of natural killer T cells by apoptosis following infection with
464 lymphocytic choriomeningitis virus. *Journal of virology*.
465 2001;75(22):10746-54.
- 466 30. Sandberg JK, Fast NM, Palacios EH, Fennelly G, Dobroszycki J, Palumbo P,
467 Wiznia A, Grant RM, Bhardwaj N, Rosenberg MG, et al. Selective loss of
468 innate CD4(+) V alpha 24 natural killer T cells in human immunodeficiency

- 469 virus infection. *Journal of virology*. 2002;76(15):7528-34.
- 470 31. van der Vliet HJ, von Blomberg BM, Hazenberg MD, Nishi N, Otto SA, van
471 Benthem BH, Prins M, Claessen FA, van den Eertwegh AJ, Giaccone G, et al.
472 Selective decrease in circulating V alpha 24+V beta 11+ NKT cells during
473 HIV type 1 infection. *Journal of immunology*. 2002;168(3):1490-5.
- 474 32. Lucas M, Gadola S, Meier U, Young NT, Harcourt G, Karadimitris A, Coumi
475 N, Brown D, Dusheiko G, Cerundolo V, et al. Frequency and phenotype of
476 circulating Valpha24/Vbeta11 double-positive natural killer T cells during
477 hepatitis C virus infection. *Journal of virology*. 2003;77(3):2251-7.
- 478 33. Lin Y, Roberts TJ, Wang CR, Cho S, and Brutkiewicz RR. Long-term loss of
479 canonical NKT cells following an acute virus infection. *European journal of*
480 *immunology*. 2005;35(3):879-89.
- 481 34. Ahmadi P, Hartjen P, Kohsar M, Kummer S, Schmiedel S, Bockmann JH,
482 Fathi A, Huber S, Haag F, and Schulze Zur Wiesch J. Defining the
483 CD39/CD73 Axis in SARS-CoV-2 Infection: The CD73(-) Phenotype
484 Identifies Polyfunctional Cytotoxic Lymphocytes. *Cells*. 2020;9(8).
- 485 35. Odak I, Barros-Martins J, Bosnjak B, Stahl K, David S, Wiesner O, Busch M,
486 Hoeper MM, Pink I, Welte T, et al. Reappearance of effector T cells is
487 associated with recovery from COVID-19. *EBioMedicine*. 2020;57(102885).
- 488 36. Zhang JY, Wang XM, Xing X, Xu Z, Zhang C, Song JW, Fan X, Xia P, Fu JL,
489 Wang SY, et al. Single-cell landscape of immunological responses in patients
490 with COVID-19. *Nature immunology*. 2020.
- 491

492 **Table 1. Baseline characteristics of the Chinese cohort.**

Parameter	Unexposed individuals	Convalescent individuals
n	21	30
Gender (M/F)	3/18	3/27
Age	33.5	36.8
Mild cases %	/	16.67% (5/30)
Moderate cases %	/	83.33% (25/30)
Days from diagnosis	/	112 (60-136)
Clinical parameters		
Fever %	/	30.00% (9/30)
Respiratory symptoms %	/	43.33% (13/30)
Hospitalized %	/	43.33% (13/30)
Oxygen therapy %	/	23.33% (7/30)
Laboratory parameters		
Leukopenia %	/	43.48% (10/23)
Lymphopenia %	/	60.87% (14/23)
Increased CRP %	/	52.63% (10/19)
Increased ferritin %	/	12.50% (1/8)
Increased LDH %	/	14.29% (2/14)
Abnormal liver function %	/	42.86% (6/14)
Abnormal renal function %	/	0% (0/14)
Increased CK %	/	7.69% (1/13)

Abnormal blood coagulation %	/	38.46% (5/13)
Increased IL-6 %	/	76.92(10/13)
CT scan		
Normal %	/	16.67% (5/30)
Viral pneumonia %	/	83.33% (25/30)
Virological markers		
RNA positive %	/	43.33% (13/30)
IgM single positive %	/	0.00% (0/30)
IgG single positive %	/	80.00% (24/30)
IgM & IgG positive %	/	20.00% (6/30)
IgG turning negative %	/	10% (3/30)
Neutralizing antibody %	/	90% (27/30)

493

494

495

496

497

498

499

500

501

502 **Table 2. Baseline characteristics of the German cohort.**

Parameter	Unexposed individuals	Convalescent individuals
n	6	19
gender (M/F)	2/4	10/9
age (mean)	46.3	44.8
Hospitalized %		10.53% (2/19)
RNA positive	/	47.37% (9/19)
Anti-SARS-CoV-2 IgA and/or IgG positive*	/	94.74% (18/19)

*OD ratio ≥ 1.1 for IgA and IgG was considered positive (EUROIMMUN ELISA); index (S/C) ≥ 1.4 is considered positive (Abbott CMIA)

503 **Figure legends**

504 **Figure 1. Characterization of immune cell subsets in individuals recovering from**
505 **COVID-19.** (A) The fold changes of the percentages (median) of total T cells, CD4
506 and CD8 T cells, B cells, NK cells, NKT-like cells, dendritic cells, and monocytes in
507 the blood of CI (n=30) compared to those of UI (n=21) are depicted by radar plots. (B)
508 The percentages of total T cells, CD4 and CD8 T cells, B cells, NK cells, and
509 monocytes in the blood of UI (n=21) and CI (n=30) were analyzed by flow cytometry.
510 (C) The absolute numbers and percentages of NKT-like cells in the blood of UI (n=21)
511 and CI (n=30) were analyzed by flow cytometry. (D) The percentages of invariant
512 NKT (iNKT) cells in the blood of UI (n=6) and CI (n=19) were analyzed by flow
513 cytometry. (E) The absolute numbers and percentages of dendritic cells in the blood of
514 UI (n=21) and CI (n=30) were analyzed by flow cytometry. CI: COVID-19
515 convalescent individuals, UI: SARS-CoV-2-unexposed individuals. Black and blue
516 lines in the figures: median and quartiles. Statistically significant differences are
517 indicated by asterisks (* < 0.05, ** < 0.01; Non-parametric Mann-Whitney test).

518

519 **Figure 2. Characterization of immune cell death in individuals recovering from**
520 **COVID-19.** (A) The percentages of early apoptosis (Annexin V+ 7-AAD-) and late
521 apoptosis / necroptosis (Annexin V+ 7-AAD+) of NKT-like cells in the blood of CI
522 (n=30) compared to those of UI (n=21) were analyzed by flow cytometry. (B)
523 Correlation analysis between the frequencies and the late apoptosis / necroptosis of

524 NKT-like cells was performed in CI. (C) The percentages of early apoptosis (Annexin
525 V+ 7-AAD-) and late apoptosis / necroptosis (Annexin V+ 7-AAD+) of CD4 T, CD8
526 T, B, and NK cells in the blood of CI (n=30) compared to those of UI (n=21) were
527 analyzed by flow cytometry. CI: COVID-19 convalescent individuals, UI:
528 SARS-CoV-2-unexposed individuals. Black and blue lines in the figures: median and
529 quartiles. Statistically significant differences are indicated by asterisks (* < 0.05, ** <
530 0.01; Non-parametric Mann-Whitney test).

531

532 **Figure 3. Characterization of T cell phenotypes in the PBMCs of individuals**
533 **recovering from COVID-19.** (A) The percentages of Ki67+ CD4 and CD8 T cells in
534 the blood of UI (n=21) and CI (n=30) were analyzed by flow cytometry. (B) and (C)
535 The fold changes of the percentages (median) of CD38+ HLA-DR-, CD38-
536 HLA-DR+, CD38+ HLA-DR+, PD-1+ TOX-, PD-1- TOX+, PD-1+ TOX+, and
537 TIM-3+ CD4 and CD8 T cells in the blood of CI (n=30) compared to those of UI
538 (n=21) are depicted by radar plots. (D) The percentages of TIM-3+ CD4 and CD8 T
539 cells in the blood of UI (n=21) and CI (n=30) were analyzed by flow cytometry. (E)
540 The percentages of Foxp3+ CD4 T cells in the blood of UI (n=21) and CI (n=30) were
541 analyzed by flow cytometry. CI: COVID-19 convalescent individuals, UI:
542 SARS-CoV-2-unexposed individuals. Black and blue lines in the figures: median and
543 quartiles. Statistically significant differences are indicated by asterisks (* < 0.05, ** <
544 0.01; Non-parametric Mann-Whitney test).

545

546 **Figure 4. Characterization of cytotoxic and cytokine profiles of T, NK and**
547 **NKT-like cells in the PBMCs of individuals recovering from COVID-19.** (A) The
548 fold changes of the percentages (median) of Granzyme B, perforin, IFN- γ , IL-6 and
549 GM-CSF producing NKT-like cells in the blood of CI compared to those of UI are
550 depicted by radar plots. (B) The percentages and MFI (Geometric mean) of Granzyme
551 B expression of NKT-like cells in the blood of UI (n=16) and CI (n=25) were
552 analyzed by flow cytometry. (C) The fold changes of the percentages (median) of
553 Granzyme B, perforin, IFN- γ , IL-6 and GM-CSF producing CD8 T cells in the blood
554 of CI compared to those of UI are depicted by radar plots. (D) The percentages and
555 MFI (Geometric mean) of Granzyme B expression of CD8 T cells in the blood of UI
556 (n=21) and CI (n=30) were analyzed by flow cytometry. (E) The fold changes of the
557 percentages (median) of Granzyme B, perforin, IFN- γ , IL-6 and GM-CSF producing
558 CD4 T cells in the blood of CI compared to those of UI are depicted by radar plots. (F)
559 The percentages and MFI (Geometric mean) of Granzyme B expression of CD4 T
560 cells in the blood of UI (n=21) and CI (n=30) were analyzed by flow cytometry. CI:
561 COVID-19 convalescent individuals, UI: SARS-CoV-2-unexposed individuals. Black
562 and blue lines in the figures: median and quartiles. Statistically significant differences
563 are indicated by asterisks (* < 0.05, ** < 0.01; Non-parametric Mann-Whitney test).

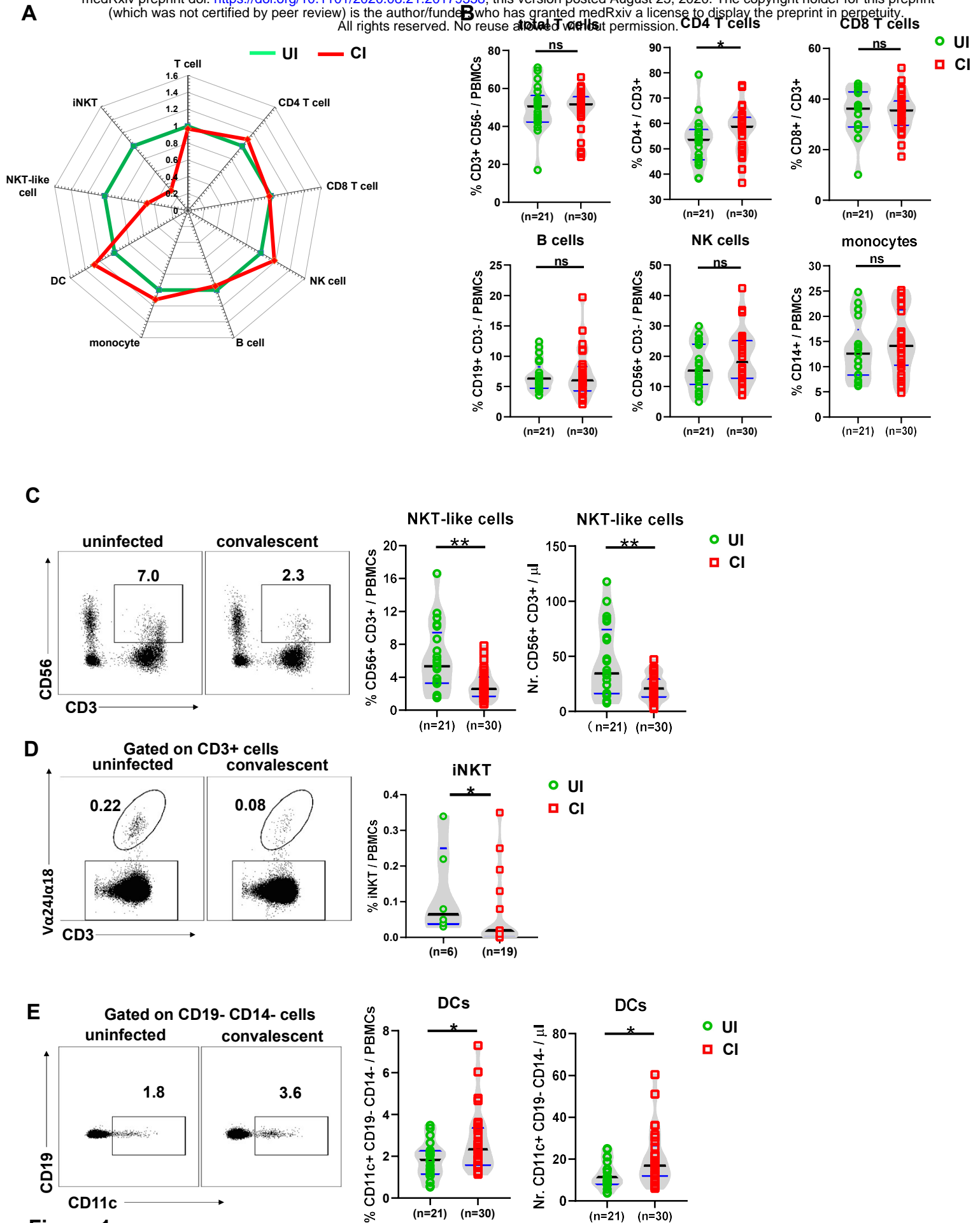
564

565 **Figure 5. Characterization of the effector function of CD4 and CD8 T cells in the**

566 **PBMCs of individuals recovering from COVID-19.** PBMCs of UI (n=5) and CI
567 (n=5) were either stimulated with anti-CD3 and anti-CD28 antibodies (α CD3/CD28)
568 or left unstimulated (UC) and cultured for 5 days. The percentages Ki67 (A), IFN- γ
569 (B), IL-2 (C), and TNF- α (D) positive CD4 (left) and CD8 (right) T cells were
570 analyzed by flow cytometry. CI: COVID-19 convalescent individuals, UI:
571 SARS-CoV-2-unexposed individuals. Statistically significant differences are indicated
572 by asterisks (* < 0.05, ** < 0.01; Non-parametric Mann-Whitney test).

573

574 **Figure 6. Characterization of phenotypes of antigen presenting cells in the**
575 **PBMCs of individuals recovering from COVID-19.** (A) The fold changes of the
576 MFI (Geometric mean) of CD80, CD86, CD72, and PD-L1 expression on DCs in the
577 blood of CI (n=30) compared to those of UI (n=21) are depicted by radar plots. (B)
578 The MFI (Geometric mean) of CD80 expression on DCs in the blood of UI (n=21)
579 and CI (n=30) were analyzed by flow cytometry. (C) The fold changes of the MFI
580 (Geometric mean) of CD80, CD86, CD72, and PD-L1 expression on B cells in the
581 blood of CI (n=30) compared to those of UI (n=21) are depicted by radar plots. (D)
582 The MFI (Geometric mean) of CD80, CD72 and PD-L1 expression on DCs in the
583 blood of UI (n=21) and CI (n=30) were analyzed by flow cytometry. CI: COVID-19
584 convalescent individuals, UI: SARS-CoV-2-unexposed individuals. Black and blue
585 lines in the figures: median and quartiles. Statistically significant differences are
586 indicated by asterisks (* < 0.05, ** < 0.01; Non-parametric Mann-Whitney test).



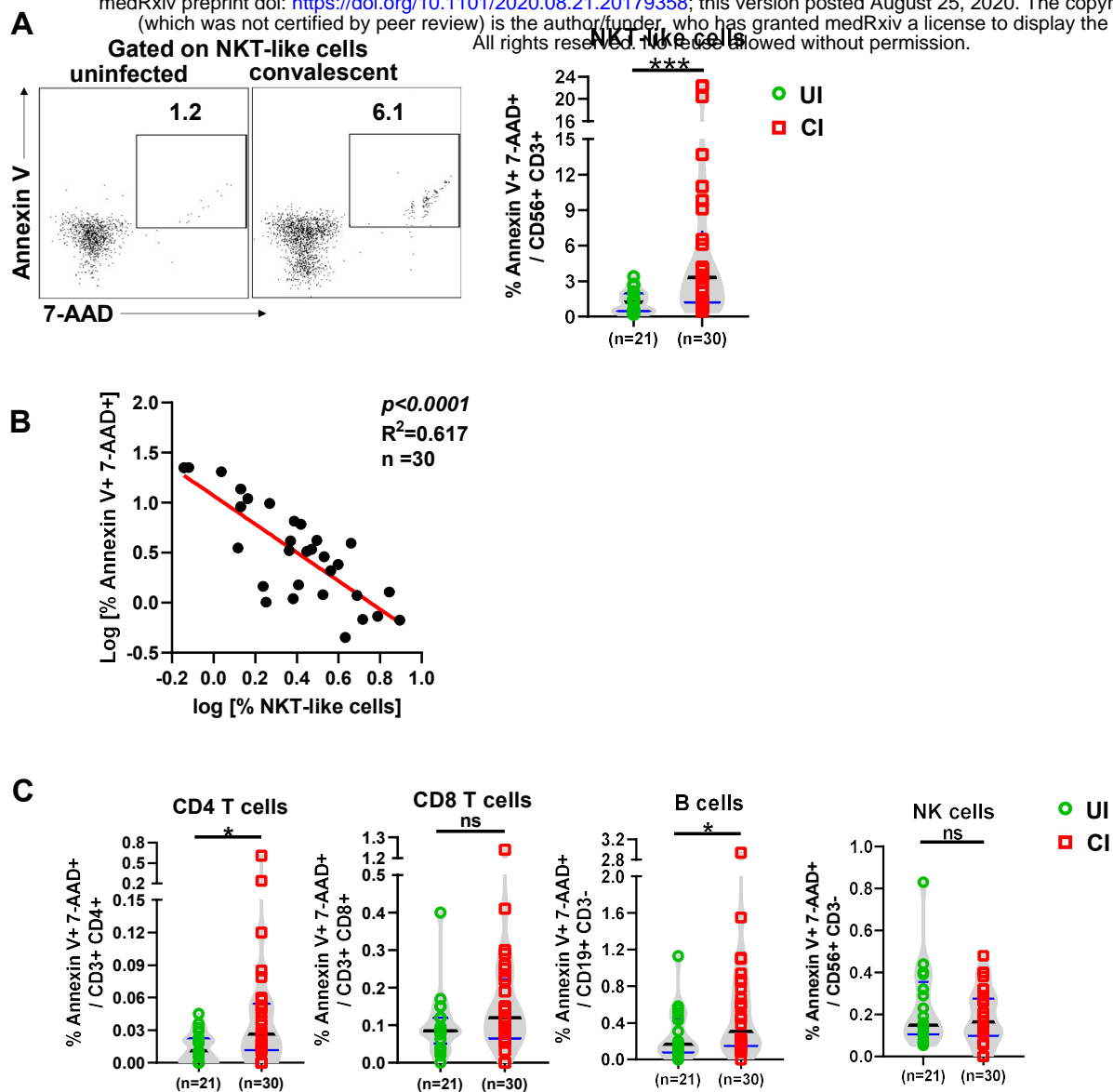


Figure 2

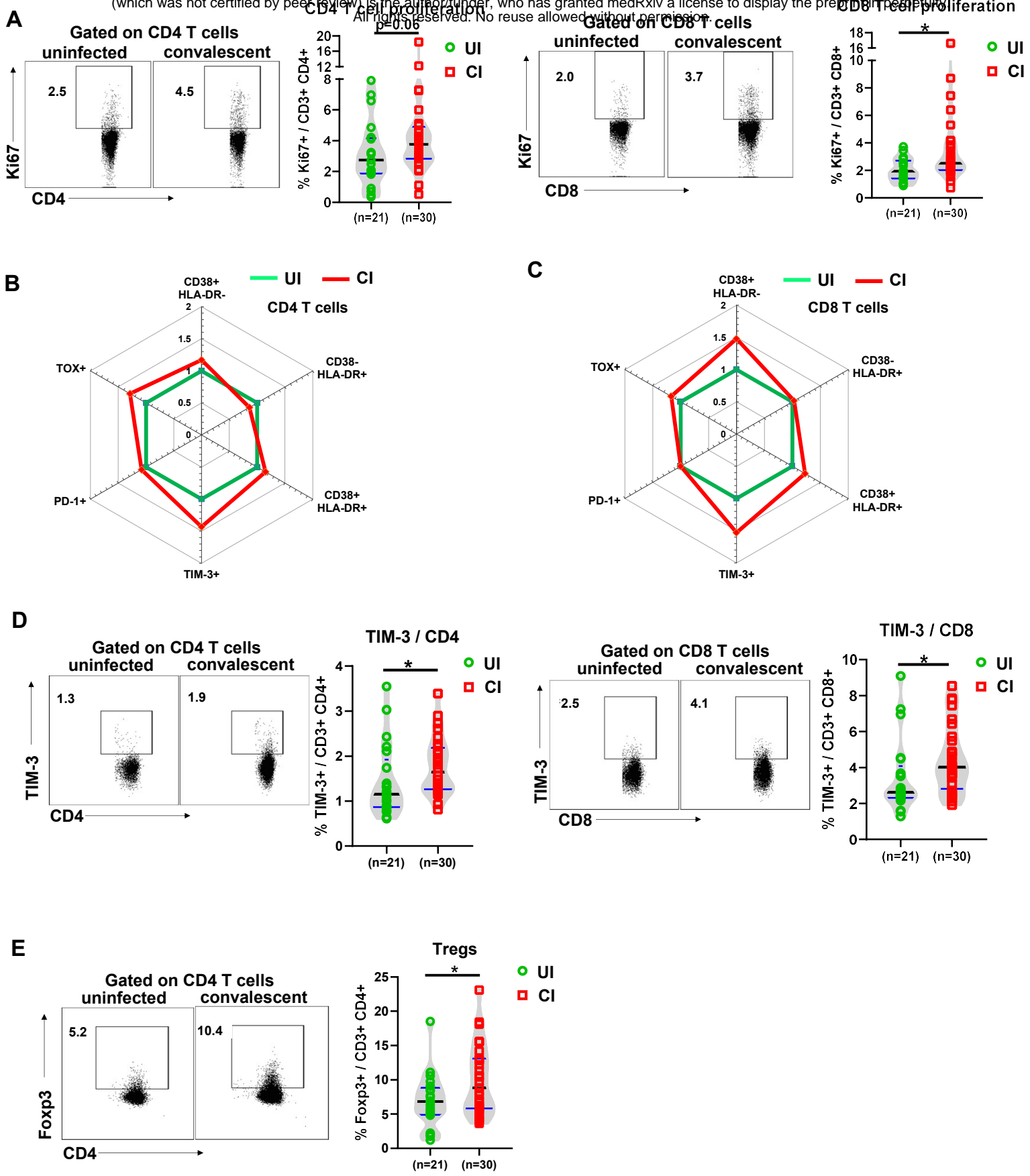
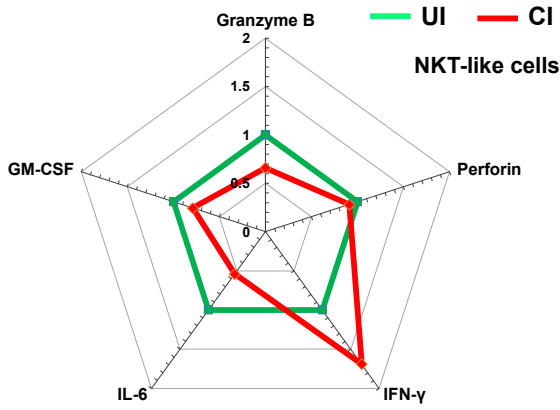
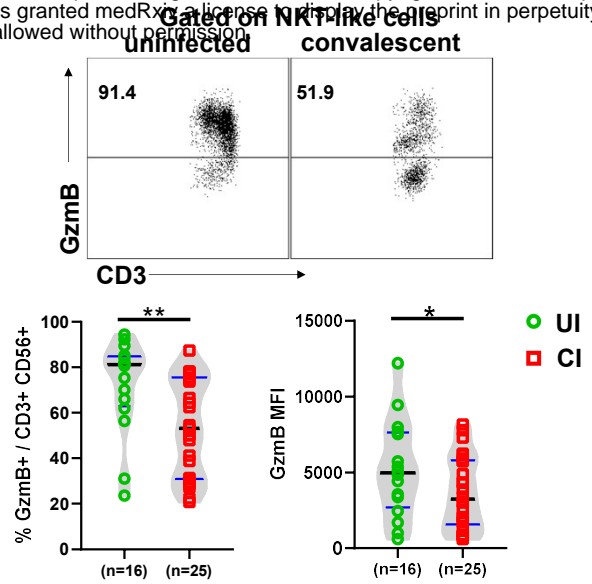


Figure 3

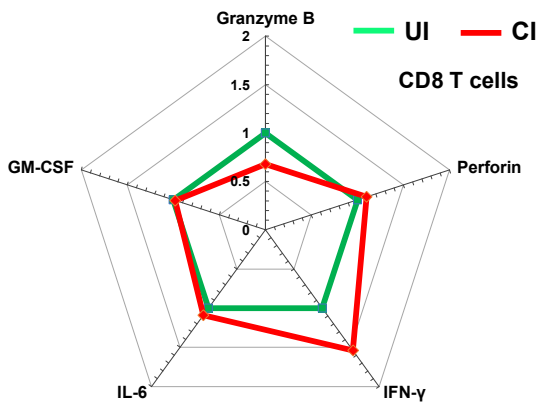
A



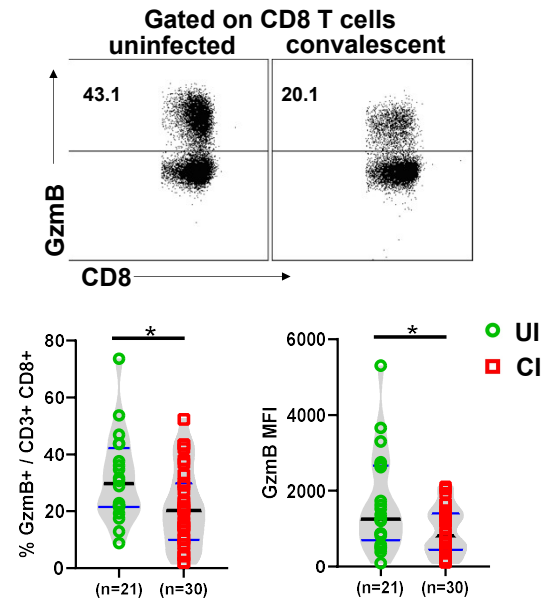
B



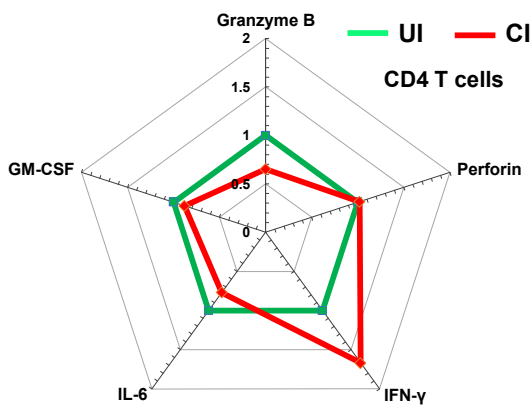
C



D



E



F

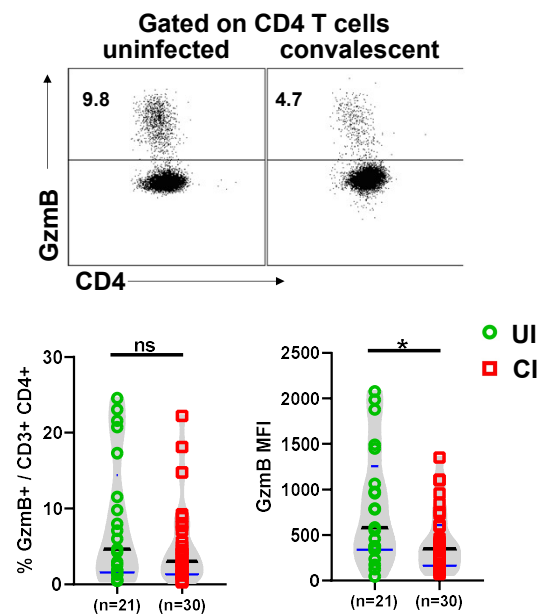


Figure 4

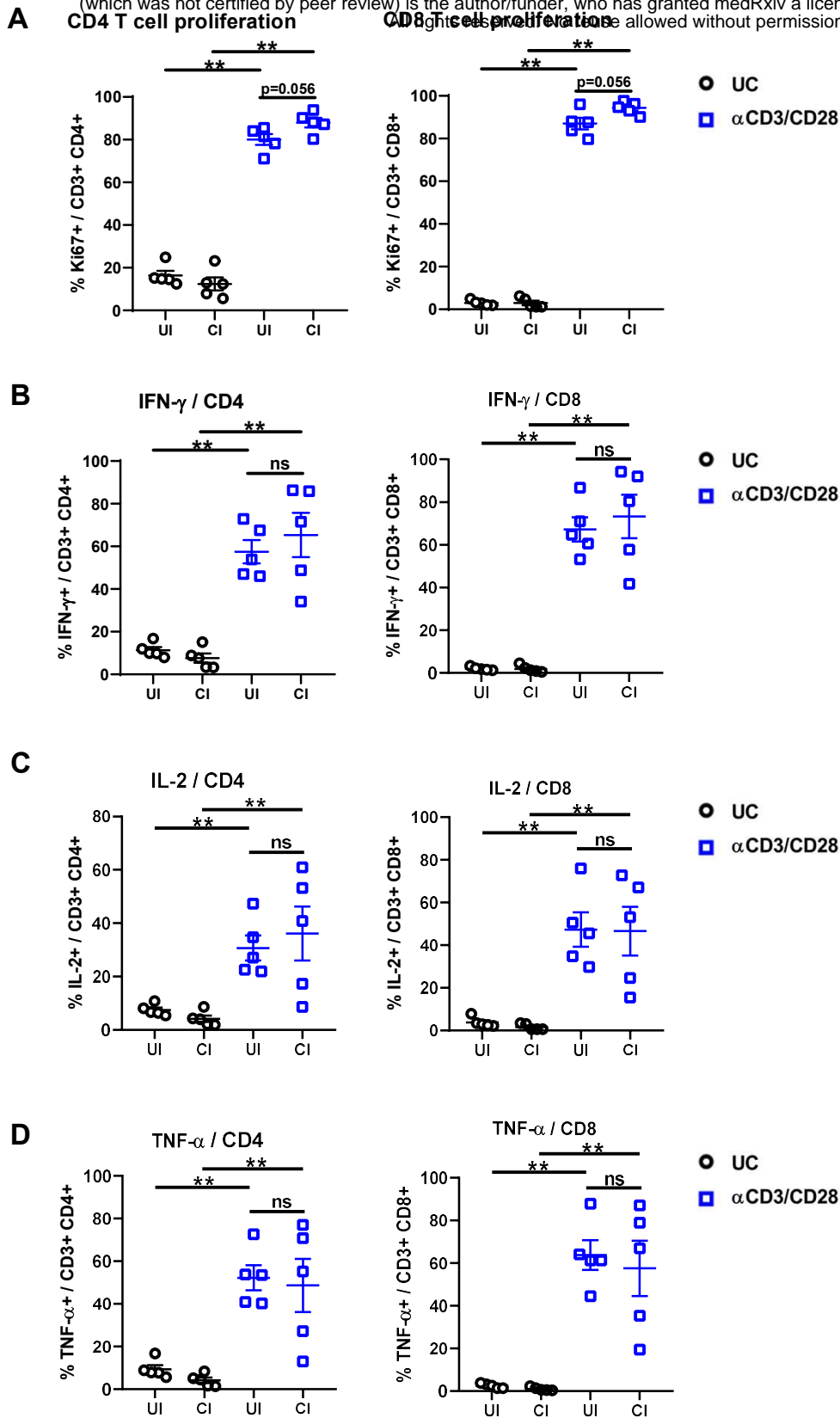
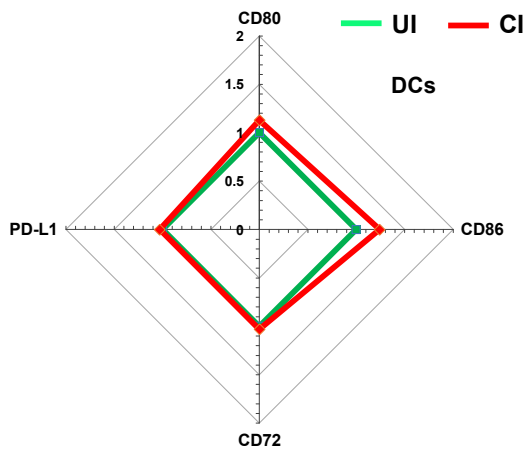
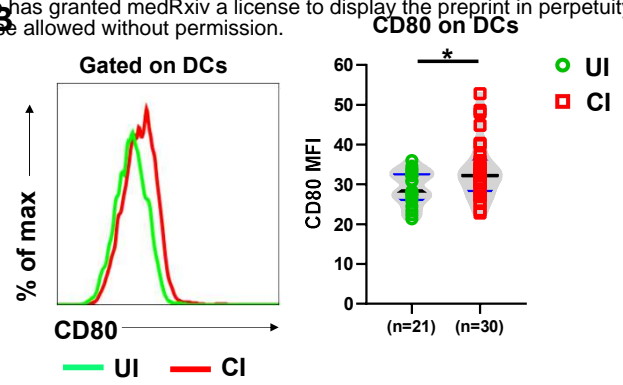


Figure 5

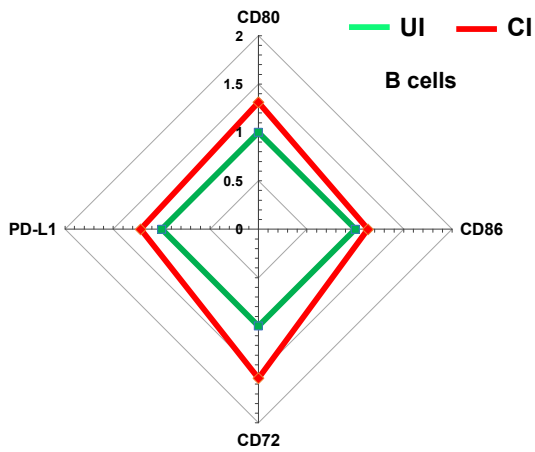
A



B



C



D

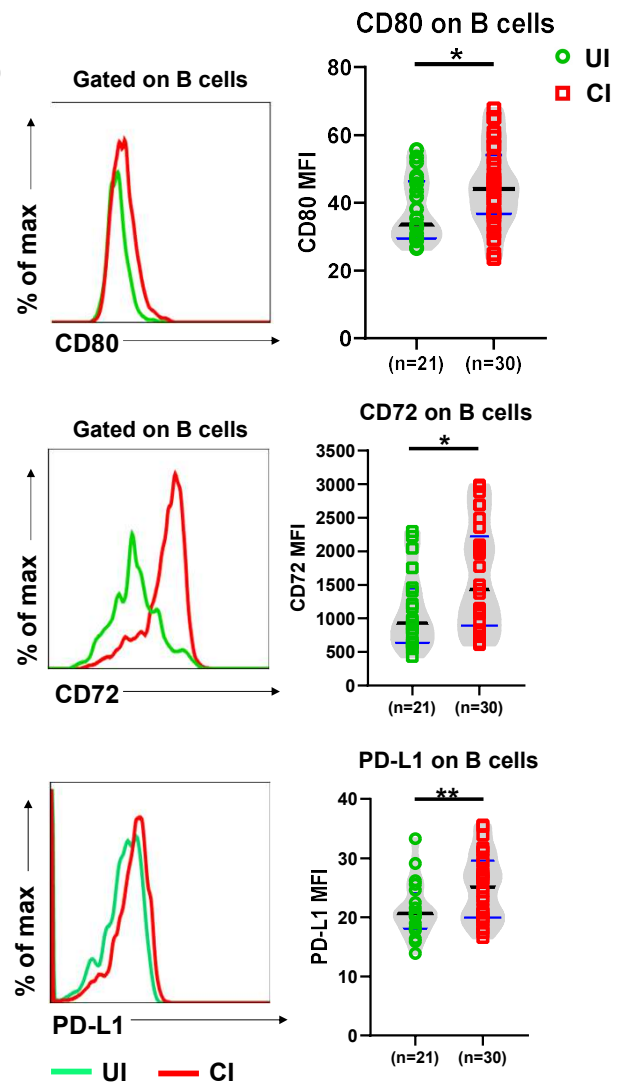


Figure 6